

Magnetic transitions in Dy-microalloyed Fe-based bulk metallic glasses

Y H Zhao¹, M X Pan¹, D Q Zhao¹, W H Wang^{1,3} and J Eckert²

¹ Institute of Physics, Chinese Academy of Sciences, Beijing 100080, People's Republic of China

² Technische Universität Darmstadt, FG Material- und Geowissenschaften, FG Physikalische Metallkunde, Petersenstraße 23, D-64287 Darmstadt, Germany

E-mail: whw@aphy.iphy.ac.cn

Received 13 February 2005, in final form 29 April 2005

Published 17 June 2005

Online at stacks.iop.org/JPhysD/38/2162

Abstract

The magnetic properties of $\text{Fe}_{70-x}\text{Dy}_x\text{Zr}_8\text{Mo}_5\text{W}_2\text{B}_{15}$ ($0 \leq x \leq 5$) bulk metallic glasses (BMGs) are studied using dc and ac susceptibility measurements. A re-entrant spin glass behaviour is observed in the BMGs and the phenomenon is ascribed to Dy-microalloying-induced site frustration. The magnetic properties of the BMGs are found to be tunable by appropriate selection of the Dy content, and the schematic magnetic phase diagram as a function of Dy content is derived.

Addition of large atoms, which have a large negative heat of mixing with other components, will increase the atomic size mismatches among the components, destabilize the competing crystalline and stabilize the liquid phase and thus enhance the glass-forming ability (GFA) of alloys [1–5]. For example, in Fe-based alloys, an appropriate minor Y/Ln alloying addition is effective for improving the GFA [6, 7]. The Fe-based bulk metallic glasses (BMGs) which exhibit high corrosion resistance, high specific strength and hardness and good magnetic properties have attracted much attention for potential applications as advanced materials [8–10]. The rare earth elements are magnetic owing to their partially filled inner f electron shells. Hence, minor additions of magnetic rare earth elements may affect not only the GFA of bulk glass-forming alloys but also their magnetic properties.

In this work, we have studied the effects of minor Dy addition on the magnetic properties of a $\text{Fe}_{70}\text{Zr}_8\text{Mo}_5\text{W}_2\text{B}_{15}$ BMG. A re-entrant spin-glass (RSG) behaviour is observed in the Dy microalloyed alloys. Their magnetic properties are found to be tunable by appropriate selection of Dy content, and a schematic magnetic phase diagram of the alloy is obtained.

The $\text{Fe}_{70-x}\text{Dy}_x\text{Zr}_8\text{Mo}_5\text{W}_2\text{B}_{15}$ ($0 \leq x \leq 5$) alloys with the nominal compositions were prepared by arc melting the mixture of pure elements (better than 99.95 at%) of Fe, Zr, Mo, W, B and Dy. The master alloys were remelted several times for homogenization and the melt was suction-cast into a Cu mould under argon atmosphere to get

cylindrical rods of 1–3 mm diameter. The structure of the samples was characterized by x-ray diffraction (XRD) using a MAC M03 XHF diffractometer with Cu K_α radiation. Thermal analysis was carried out in a Perkin–Elmer DTA-7 differential temperature analyser (DTA) with a heating rate of 10 K min^{-1} . AC-magnetic properties and magnetization curves were measured using a Quantum Design Inc. PPMS 6600 physical properties measurement system in the temperature range of 2–350 K with an ac magnetic field of 10 Oe and a frequency of 1000 Hz. The M–H curves were measured with an applied field $\mu_0 H = 4 \text{ T}$ at different temperatures. Static susceptibilities of zero-field-cooling (ZFC) and field-cooling (FC) measurements were carried out in two ways: first, the sample was cooled from 350 to 2 K without any magnetic field and then heated back to 350 K under 250 Oe (ZFC curve); afterwards, the sample was cooled again to 2 K without removing the field, and the magnetization was measured while heating back to 350 K, following the same steps as before (FC curve).

Figure 1(a) shows the XRD patterns of the as-cast 2 mm diameter $\text{Fe}_{70-x}\text{Dy}_x\text{Zr}_8\text{Mo}_5\text{W}_2\text{B}_{15}$ ($0 \leq x \leq 5$) alloys with different Dy contents. The patterns of all samples consist mainly of broad diffraction maxima, indicating an amorphous structure and no appreciable diffraction peaks corresponding to crystalline phases can be detected within the resolution limits of the XRD measurements. The positions of the broad XRD maxima which provide information for the nearest-neighbour distance show that alloys have similar highly random packed structure. The shift of the positions

³ Author to whom any correspondence should be addressed.

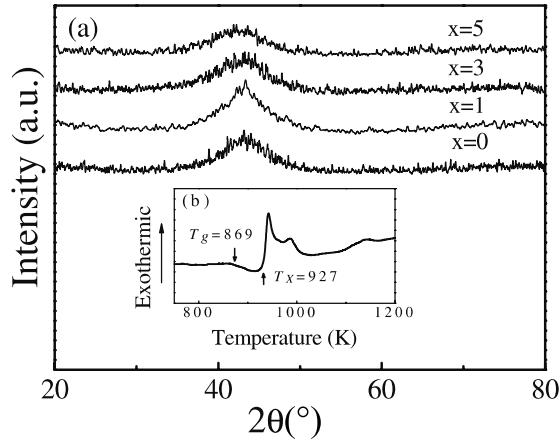


Figure 1. (a) XRD patterns of as-cast $\text{Fe}_{70-x}\text{Dy}_x\text{Zr}_8\text{Mo}_5\text{W}_2\text{B}_{15}$ ($0 \leq x \leq 5$) alloys; (b) is the DTA curves of crystallization and melting of the $\text{Fe}_{70}\text{Zr}_8\text{Mo}_5\text{W}_2\text{B}_{15}$ alloy. The glass transition temperature T_g , crystallization temperature T_x are 869 K and 927 K, respectively.

of the broad XRD maxima indicates that the microstructure of the alloys have been changed by addition. However, the high resolution transmission electron microscopy observation (not shown here) indicates that little precipitation (<10%) of the ultra-fine nanocrystalline α -Fe particles with grain size of about 3–4 nm homogeneously dispersed in the amorphous matrix, which could not be detected by XRD. Figure 1(b) shows DTA curves of the $\text{Fe}_{70}\text{Zr}_8\text{Mo}_5\text{W}_2\text{B}_{15}$ alloy recorded at a heating rate of 10 K min^{-1} . An obvious glass transition and distinct crystallization events confirm the glassy structure of the as-cast alloys.

The temperature-dependent ac susceptibilities of the BMGs under a field of $7.96 \times 10^2 \text{ A m}^{-1}$ (10 Oe) at 1 kHz are shown in figure 2. With decreasing temperature, the real component of the ac susceptibility, χ' of the $\text{Fe}_{70}\text{Zr}_8\text{Mo}_5\text{W}_2\text{B}_{15}$ BMG, exhibits a rapid increase at about 223 K which corresponds to the Curie temperature, T_C . Above T_C , the value of χ' is nearly zero, below T_C , χ' remains almost unchanged with decreasing temperature down to 2 K. This behaviour indicates that the BMG is paramagnetic at room temperature and becomes ferromagnetic below 223 K. An ordinary paramagnetic (PM) to ferromagnetic (FM) transition occurs in the undoped BMG. With only 1 at% Dy addition, the temperature-dependent χ' curve is obviously changed as shown in figure 2. There are two knees in the χ' - T curve: the first at a high temperature of around 233 K is sharp and corresponds to a PM-FM transition, and the second one at a low temperature of around 60 K results from an FM to spin glass (SG) transition. There exists a plateau between the two knees. The χ' - T curve of the BMG shows the behaviour of classical RSG [11]. With increasing Dy content, the FM to SG transition temperature, T_f , increases and the width of the plateau shrinks. For the $\text{Fe}_{65}\text{Zr}_8\text{Mo}_5\text{W}_2\text{B}_{15}\text{Dy}_5$ alloy, T_C and T_f are around 167 K and 216 K, respectively.

The temperature dependences of the ZFC-FC susceptibilities of the BMGs at $1.99 \times 10^4 \text{ A m}^{-1}$ (250 Oe) are shown in figure 3. The ZFC and FC susceptibilities of the $\text{Fe}_{70}\text{Zr}_8\text{Mo}_5\text{W}_2\text{B}_{15}$ BMG are not separated. However, the temperature dependence of the ZFC susceptibility of

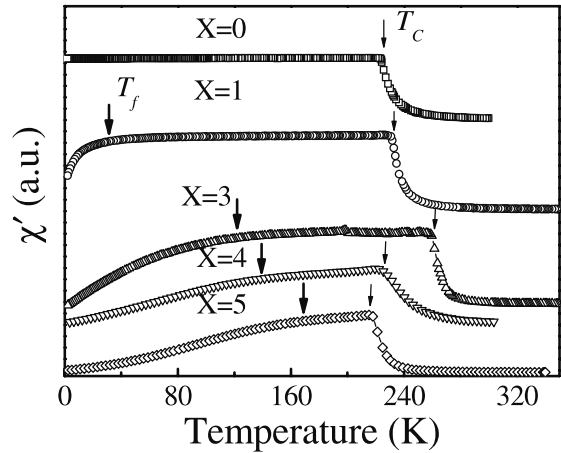


Figure 2. Temperature-dependent χ' for the $\text{Fe}_{70-x}\text{Dy}_x\text{Zr}_8\text{Mo}_5\text{W}_2\text{B}_{15}$ ($0 \leq x \leq 5$) alloys at an applied field $7.96 \times 10^2 \text{ A m}^{-1}$ (10 Oe) and a frequency of 1000 Hz. T_C and T_f are the transition temperature from paramagnetism to ferromagnetism and from ferromagnetism to spin glass, respectively.

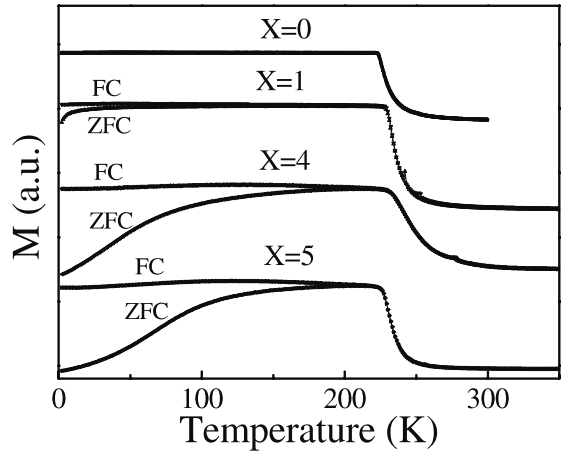


Figure 3. Temperature dependence of the ZFC-FC susceptibilities for the $\text{Fe}_{70-x}\text{Dy}_x\text{Zr}_8\text{Mo}_5\text{W}_2\text{B}_{15}$ ($0 \leq x \leq 5$) alloys at an applied field of $1.99 \times 10^4 \text{ A m}^{-1}$ (250 Oe).

the BMG with 1 at% Dy addition becomes separated at T_f and shows a plateau and two transitions. The upper one corresponds to the PM-FM transition, and the one at low temperature corresponds to the FM-SG transition. With increasing Dy content, T_f increases and the plateau region shrinks, similar to the results of the ac susceptibility measurements. The results confirm the microalloying-induced magnetic transition in the BMGs. Because of the higher applied field $1.99 \times 10^4 \text{ A m}^{-1}$ (250 Oe) compared with the applied ac field $7.96 \times 10^2 \text{ A m}^{-1}$ (10 Oe), the FC and ZFC susceptibilities for the BMGs with higher Dy contents are not separated completely.

The M-H loops at different temperatures of $\text{Fe}_{70}\text{Zr}_8\text{Mo}_5\text{W}_2\text{B}_{15}$ BMG and $\text{Fe}_{65}\text{Zr}_8\text{Mo}_5\text{W}_2\text{B}_{15}\text{Dy}_5$ are shown in figures 4(a) and (b), respectively. For the $\text{Fe}_{70}\text{Zr}_8\text{Mo}_5\text{W}_2\text{B}_{15}$ BMG, the saturation magnetization is very low at room temperature (300 K), and the curve exhibits approximately paramagnetic behaviour. At 200 K the alloy shows soft ferromagnetism, but it is hard to achieve saturation. The M-H curves below 100 K have much easier saturation

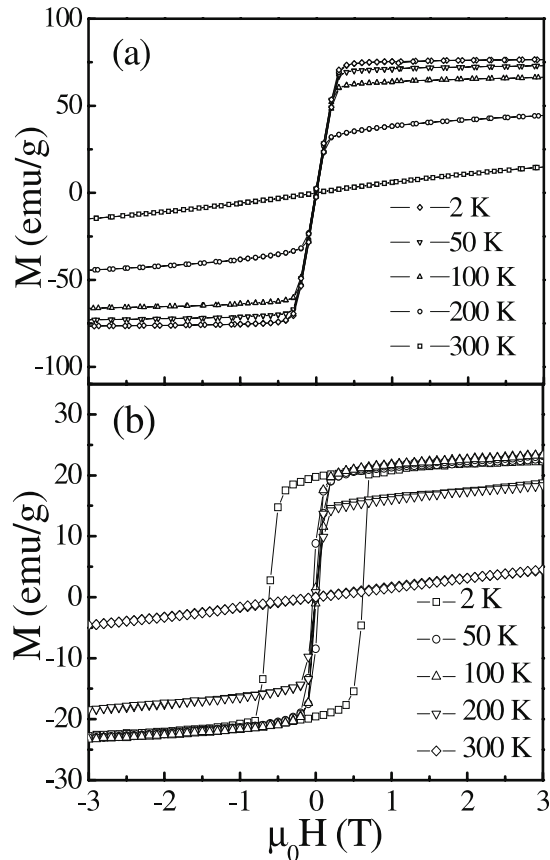


Figure 4. Magnetization loops of the $\text{Fe}_{70}\text{Zr}_8\text{Mo}_5\text{W}_2\text{B}_{15}$ (a) and $\text{Fe}_{65}\text{Dy}_5\text{Zr}_8\text{Mo}_5\text{W}_2\text{B}_{15}$ (b) BMGs at different temperatures.

than those at high temperature, and the saturation magnetization also increases with the decrease of temperature. The magnetization curve of the $\text{Fe}_{65}\text{Zr}_8\text{Mo}_5\text{W}_2\text{B}_{15}\text{Dy}_5$ BMG is similar to that of the $\text{Fe}_{70}\text{Zr}_8\text{Mo}_5\text{W}_2\text{B}_{15}$ BMG at 300 and 200 K. But the saturation magnetization remains unchanged and the coercivity increases dramatically with decreasing temperature. At 2 K, the coercivity is $H_C = 5.17 \times 10^5 \text{ A m}^{-1}$ (6500 Oe). The increase of H_C with decreasing temperature is also observed in conventional spin glass systems [11–13]. The saturation magnetization of the BMG with Dy addition is only about 22 emu g^{-1} and far lower than that of the undoped BMG (75 emu g^{-1}).

The phenomena induced by Dy microalloying can be identified as site frustration achieved by introducing a dopant with AF coupling to all its nearest neighbours [14]. With the random addition of Dy, the local electronic environment in the glassy alloys, which plays an important role in determining the basic properties of FM [15], will be changed, and the local magnetic moment of Fe will ferromagnetically or antiferromagnetically couple with the neighbouring atoms depending on the exchange pair energy [15]. For the site frustration, which depends on the matrix and dopant element [14, 15], it can only be induced for a sufficiently high doping content. The low fraction and isolated AF-coupled sites simply align antiparallel to the majority FM order and reduce the total magnetization but cause no noncollinearity. The frustration only appears when the dopant density is high enough for AF–AF pairs to occur and RSG appears [16, 17].

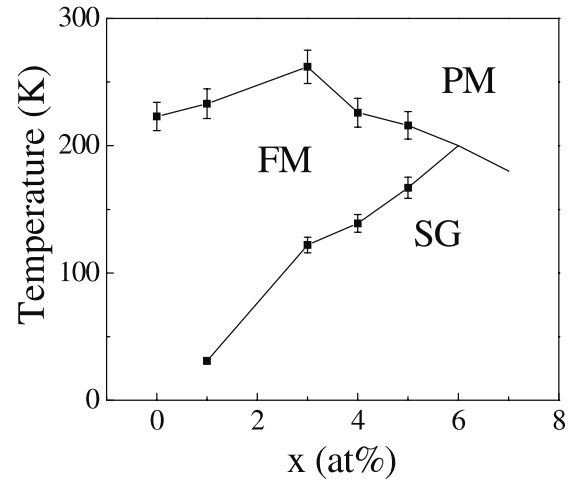


Figure 5. Magnetic phase diagram for the $\text{Fe}_{70-x}\text{Dy}_x\text{Zr}_8\text{Mo}_5\text{W}_2\text{B}_{15}$ ($0 \leq x \leq 5$) BMGs derived from the temperature-dependent ac susceptibility at $7.96 \times 10^2 \text{ A m}^{-1}$ (10 Oe) and 1000 Hz.

For the $\text{Fe}_{69}\text{Zr}_8\text{Mo}_5\text{W}_2\text{B}_{15}\text{Dy}_1$ alloy, at about 233 K, there is a PM to FM transition, and local AFM interaction exists in the FM matrix. At T_f , the frustration owing to the competition between the FM and AFM interaction leads to freezing of the spins and thus SG behaviour appears [14]. With the increase of the Dy content, the AFM region becomes larger and the increased frustration in the alloys makes them easier to freeze the spin components and thus T_f increases [14]. With the decrease in temperature, the frozen spins make the change of the direction of the magnetic moments harder. So the coercivity increases with decreasing temperature, as shown for the $\text{Fe}_{65}\text{Zr}_8\text{Mo}_5\text{W}_2\text{B}_{15}\text{Dy}_5$ alloy. Owing to the existence of the local AFM region, the reduction of the total magnetization of the alloy lowers the saturation magnetization with the increase of the Dy content as well.

We note that the observed spin-glass behaviour in the Dy-doped metallic glasses probably has its origin in the same random field interaction that was discussed in the amorphous R–Fe alloys [18–20]. In the late 1970s [18, 19] it was shown theoretically that the random crystal field anisotropy induced by the rare earth is sufficient to break the long-range exchange interaction provided by the Fe and produce a spin-glass-like magnetic state. Experimental studies of FeTb metallic glasses [20] showed that even for 0.02 Tb addition, long-range order was effectively destroyed by the random crystal field interaction of the rare earth ions.

The above magnetic data for the BMGs derived from temperature-dependent ac susceptibility measurements at $7.96 \times 10^2 \text{ A m}^{-1}$ (10 Oe) and 1000 Hz can be summarized in a schematic magnetic phase diagram, as shown in figure 5. According to this diagram, one can prepare alloys with specific properties by appropriate selection of the Dy microalloying concentration.

In conclusion, the magnetic properties of $\text{Fe}_{70-x}\text{Zr}_8\text{Mo}_5\text{W}_2\text{B}_{15}\text{Dy}_x$ ($0 \leq x \leq 5$) BMGs are tunable by appropriate selection of the microalloying Dy content. With the change of the Dy content, a PM to FM transition and an FM to spin glass transition are observed in the BMGs. The RSG behaviour is ascribed mainly to the site frustration induced by Dy microalloying.

Acknowledgments

The financial support provided by the National Science Foundation of China (Grants No 50321101) and the Chinesisch–Deutsches Zentrum für Wissenschaftsförderung (Grant No GZ032/7) as well as the Deutsche Forschungsgemeinschaft (Grant Ec 111/12-1) is gratefully acknowledged.

References

- [1] Richman M H 1967 *An Introduction to Physical Metallurgy* (Massachusetts: Blaisdell) p 215
- [2] Hu Y, Pan M X, Zhao Y H and Wang W H 2003 *Mater. Lett.* **57** 2698
- [3] Wang W H, Bian Z, Wen P and Zhang Y 2002 *Intermetallics* **10** 1249
- [4] Wang W H, Dong C and Shek C H 2004 *Mater. Sci. Eng. R* **44** 45
Zhang Y and Wang W H 2000 *Mater. Trans.* **41** 1410
- [5] Wang W H, Wei Q and Bai H Y 1997 *Appl. Phys. Lett.* **71** 58
- [6] Lu Z P, Liu C T and Porter W D 2003 *Appl. Phys. Lett.* **83** 2581
- [7] Ponnambalam V, Poon S J and Shiflet G J 2004 *J. Mater. Res.* **19** 1320
- [8] Fu H and Mansuripur M 1992 *Phys. Rev. B* **45** 7188
- [9] Inoue A, Yoshida H and Itoi T 1999 *Bulk Metallic Glasses* ed W L Johnson *et al* (*Material Research Society Symp. Proc.* (Warrendale, PA, 1999) vol 554) pp 251–62
- [10] Ponnambalam V, Poon S J and Shiflet G J 2003 *Appl. Phys. Lett.* **83** 1131
- [11] Binder K and Young A P 1986 *Rev. Mod. Phys.* **58** 801
- [12] Dho J, Dim W S and Hur N H 2002 *Phys. Rev. Lett.* **89** 027202
- [13] Campbell I A, Senoussi S and Varret F 1983 *Phys. Rev. Lett.* **50** 1615
- [14] Nielsen M, Ryan D H, Guo H and Zuckermann M 1996 *Phys. Rev. B* **53** 343
- [15] Kakehashi Y 1991 *Phys. Rev. B* **43** 10820
- [16] Wang F, Zhang J and Chen Y F 2004 *Phys. Rev. B* **69** 094424
- [17] Ryan D H, Beath A D and McCalla E 2003 *Phys. Rev. B* **67** 104404
- [18] Cochrane R W, Harris R and Zuckermann M J 1978 *Phys. Rep.* **48** 476
- [19] Pelcovits R A, Pytte E and Rudnick J 1980 *Phys. Rev. Lett.* **40** 476
- [20] Rhyne J J 1986 *Physica B* **136** 30